https://doi.org/10.5194/egusphere-2026-5120
Preprint. Discussion started: 24 September 2026

Simultaneous, in situ detection of gas-phase carbon disulfide (CS_2) and carbonyl sulfide (OCS) via O_2^+ chemical ionization mass spectrometry

Elisabeth N. Kray[1], Delaney B. Kilgour[1,a], Martina N. Rogers[1,b], Christopher M. Jernigan[1,c], Michael P. Vermeuel[1,d], Timothy H. Bertram[1]

[1]Department of Chemistry, University of Wisconsin-Madison, Madison, WI 53706, USA

[a] now at: Physicians, Scientists, and Engineers for Healthy Energy, Oakland, California 94612, USA

[b] now at: Minnesota Pollution Control Agency, Saint Paul, MN 55155, USA

[c] now at: Office of Research and Development, U.S. Environmental Protection Agency, Research Triangle Park, North Carolina 27711, USA

[d] now at: Department of Earth, Atmospheric, and Planetary Sciences, Purdue University, West Lafayette, IN 47907, USA

Correspondence to: Timothy H. Bertram (timothy.bertram@wisc.edu)

Abstract

Carbonyl sulfide (OCS) is the largest gas-phase sulfur reservoir in the troposphere. OCS is both directly emitted to the atmosphere and formed chemically in the atmosphere following the oxidation of reduced sulfur species such as carbon disulfide (CS_2) and dimethyl sulfide (C_2H_6S, DMS). OCS is the largest continuous contributor to stratospheric sulfate aerosol and a key diagnostic for the photosynthetic uptake of carbon dioxide (CO_2). Despite its importance to the OCS budget, *in situ* measurements of CS_2 are extremely limited. Here, we describe a new technique for the simultaneous measurement of CS_2, OCS, and DMS utilizing O_2^+ chemical ionization time-of-flight mass spectrometry (O_2^+ CI-ToFMS). We highlight the utility of the measurement through the reanalysis of three distinct data sets taken in remote marine, remote continental, and urban environments. We report mean CS_2 mixing ratios for the Eastern North Atlantic (2.2 ppt) and Downtown Chicago, IL (9.5 ppt), while CS_2 was not detected in Northern Wisconsin. In the Eastern North Atlantic, CS_2 showed limited temporal variability during the summer. In Chicago, CS_2 was highly variable, with episodic large enhancements (>85 ppt) suggesting local, anthropogenic sources. Results of laboratory measurements and success in the quantification of field measurements suggest that primary and secondary O_2^+ CI-ToFMS is suitable for simultaneous, *in situ* detection of CS_2 and OCS.

https://doi.org/10.5194/egusphere-2026-5120
Preprint. Discussion started: 24 September 2026

1. Introduction

Reduced sulfur gases, such as carbon disulfide (CS_2), carbonyl sulfide (OCS), dimethyl sulfide (C_2H_6S, DMS), and methanethiol (CH_3SH, MeSH) are often supersaturated in surface seawater, leading to a net ocean to atmosphere mass flux (Bandy et al., 1982; Lawson et al., 2020; Lennartz et al., 2017; Turner and Liss, 1985). In the atmosphere they can be oxidized to sulfur dioxide (SO_2), leading to the production of sulfate aerosols (Watts, 2000). Sulfate aerosol has been shown to impact Earth's radiative budget both directly and indirectly and provide suspended surface area to catalyze heterogeneous reactions (Kremser et al., 2016; Lennartz et al., 2017). Despite the importance of reduced sulfur gases, several key uncertainties surround their waterside production and emission rates as well as their gas-phase oxidation mechanisms. One specific area of uncertainty is the global inventory of OCS (Remaud et al., 2022). OCS has a chemical lifetime of > 35 years in the troposphere, rendering it chemically inert until it reaches the lower stratosphere where it can be photolyzed, leading to SO_2 production (Brühl et al., 2012; Kremser et al., 2016). It is currently estimated that OCS is the largest continuous contributor to stratospheric sulfate, accounting for 56 – 70% of the stratospheric aerosol budget (Brühl et al., 2012; Sheng et al., 2015). Recent revisions to the OCS global budget that account for the large measured OCS terrestrial sink suggest a missing source term of 230-800 Gg S yr^{-1} is needed to balance the tropospheric OCS budget (Sandoval-Soto et al., 2005). This missing source has been attributed to: 1) direct emission of OCS from the ocean, although recent studies based on seawater OCS measurements suggest that direct emissions of OCS account for less than 130 ± 80 Gg S yr^{-1} (Lennartz et al., 2017), 2) chemical production of OCS from the OH-oxidation of DMS, which was shown to be a high-yield product in the OH-oxidation of hydroperoxymethyl thioformate (HPMTF) and could account for between 52.9 and 680.1 Gg S yr^{-1}, where the range represents the impact of cloud processing in sequestering HPMTF and arresting OCS production (Jernigan et al., 2022), and 3) chemical production of OCS from CS_2 (Chin and Davis, 1993).

The chemical mechanism to produce OCS from the reaction of CS_2 with ·OH radicals is well constrained. The lifetime of CS_2 in respect to an average [·OH] of 1×10^6 molecules cm^{-3} is about 6 days ($k_{OH} = 2 \times 10^{-12} cm^3$ $molecule^{-1}$ s^{-1}) and represents the dominant tropospheric loss process for gas-phase CS_2 (Blake et al., 2004; Chin and Davis, 1993). Experimental and theoretical studies have shown that the product yield of OCS in the OH-oxidation of CS_2 is 81 ± 6% (Chin, 1992). Although the chemical fate of CS_2 is well constrained, direct measurements of CS_2 mixing ratios in both the surface ocean and lower troposphere are sparse, leading to significant uncertainty in CS_2 emission rates (Lennartz et al., 2017).

Globally, anthropogenic emissions are estimated to account for 52-58% of atmospheric CS_2 emissions (Chin and Davis, 1993; Guo et al., 2010). These emissions originate mainly from its use as a solvent in the production of rayon, but it is also known to be formed from carbon black production, sulfur recovery, and coal and fuel combustion (Blake et al., 2004; Guo et al., 2010). The remaining emission sources are believed to be biogenic with a large fraction of total sources

https://doi.org/10.5194/egusphere-2026-5120
Preprint. Discussion started: 24 September 2026

(27-34%) attributed to marine emissions of CS_2 (Chin and Davis, 1993; Watts, 2000). The marine production of CS_2 has been ascribed to biological processes involving phytoplankton and/or photochemical processes involving dissolved organic sulfur and photo-excited reactive intermediates (Lennartz et al., 2017; Xie et al., 1998, 1999). The remaining biogenic fraction (8-21%) is assigned to soil, wetlands, and volcanic emissions (Guo et al., 2010; Watts, 2000).

The limited database of existing gas-phase measurements of CS_2 suggest high spatial variability in CS_2 mixing ratios (Lennartz et al., 2020). For example, large enhancements in CS_2 from anthropogenic sources in Asia, with mixing ratios as high as 90 ppt, were observed in near-coastal plumes of polluted air (Blake et al., 2004). However, outside of these plumes, airborne measurements report lower mixing ratios in both marine and continental air (0.7 and 4.2 ppt, respectively; see Cooper and Saltzman, 1993).

Recently, Lennartz et al. (2020) reviewed the existing collection of marine CS_2 measurements, showing an average CS_2 seawater concentration of 15.7 pmol L^{-1} with a range of 6.1 to 15.6 pmol L^{-1} (20-80th percentile) and an average gas-phase marine boundary layer CS_2 concentration of 42.2 ppt with a range 2.5 to 275.7 ppt. Unfortunately, existing seawater and gas-phase measurements are sparse. Seawater CS_2 measurement reports are limited to eleven cruises with most being performed in the Atlantic Ocean, with sampling frequency biased towards daytime. Yet, the measurements cover several biological regimes and display seasonal and spatial variability. Gas-phase CS_2 measurements are even more sparse as they include only 1,036 individual measurements from six cruises, all of which sampled on the Atlantic Ocean, making spatial and temporal variability indiscernible. Despite the scarcity of the observations, the measurements that have been made to date highlight the importance of CS_2 to marine sulfur chemistry.

Most cited measurements of atmospheric CS_2 were completed between 1980 – 2010 (Lennartz et al., 2020). With few exceptions, these measurements were made using canister sampling and adsorbent and cryogenic trapping preconcentration, followed by GC separation and flame photometric detection (FPD), photoionization detection (PID), or electron capture detection (ECD) (**Table S1**). While sample preconcentration allows for increased sensitivity, necessary for detection at low concentrations (<10 ppt), it comes at the expense of time resolution and chemical interferences stemming from chemistry occurring along the sample lines and traps (Lennartz et al., 2020). Beyond chromatography techniques, Zhu *et al.* (2023) reported a real-time measurement for CS_2 utilizing ultraviolet spectroscopy, however the detection limit (3.81 ppb) does not permit sampling of CS_2 at atmospheric concentrations (< 50 ppt).

Real-time, high time resolution measurements of CS_2 are vital to quantifying CS_2 emissions. In the field, it is often difficult to discern emissions from anthropogenic activity and biogenic sources, especially in coastal regions (Lennartz et al., 2017). Real-time measurements with high sensitivity and low detection limits would allow for narrow source plume detection as well as simultaneous

https://doi.org/10.5194/egusphere-2026-5120
Preprint. Discussion started: 24 September 2026

detection of other species to help differentiate and identify measured emission sources. Paired with real-time waterside detection, marine flux inventories of CS_2 can be studied and utilized to increase our understanding of the CS_2 global budget (Watts, 2000). Similar detection in laboratory studies can be used to conduct controlled CS_2 production and loss studies to continue to fill gaps in our knowledge of CS_2 production and cycling (Lennartz et al., 2024).

Chemical ionization mass spectrometry (CIMS) has been used extensively for the measurement of DMS and MeSH. For example, proton transfer reaction mass spectrometry (PTR-MS) and benzene cluster cation CIMS have been shown to be both sensitive and specific detection techniques for measurement of DMS with detection limits as low as 2.6 ppt (3σ and 10 s; see Kim et al., 2016; Novak et al., 2022). Unfortunately, neither CS_2 nor OCS are detectable using PTR or benzene cluster cation CIMS. In this paper, we explore the use of O_2^+ chemical ionization for the simultaneous detection of CS_2, OCS, and DMS. The detection of CS_2 via O_2^+ ionization has been previously reported in the laboratory by Bloor *et al.* (2006) using selected ion flow tube mass spectrometry (SIFT-MS) of human breath, but its ppb-level sensitivity does not permit detection of trace atmospheric concentrations. Here, we discuss the dominant product ions formed in the O_2^+ ion molecule reactions, the required instrument resolving power to separate these species from ions at the same nominal mass, and the resulting O_2^+ CIMS sensitivity to DMS, CS_2, and OCS. We also report on the detection and quantification of CS_2 in the eastern North Atlantic and downtown Chicago, Illinois, as well as its apparent absence in rural Wisconsin.

2. Methods

2.1 Vocus proton-transfer-reaction time-of-flight mass spectrometer

Proton transfer reaction time-of-flight mass spectrometry uses H_3O^+ reagent ions to detect a wide array of volatile organic compounds (VOCs), as their MH^+ ions, with high sensitivity (parts-per-trillion) and fast time response (>1 Hz; see Krechmer et al., 2018). In this paper, we operated a Vocus time-of-flight mass spectrometer (Vocus; Aerodyne Research, Inc. and Tofwerk AG) using O_2^+ reagent ions (hereafter referred to as O_2^+ CI-ToFMS). O_2^+ reagent ions were generated by flowing 21 sccm of UHP O_2 into the discharge ion source (Norman et al., 2007). The focusing ion-molecule reactor (FIMR) was operated at 1.5 mbar, 100°C, and at a voltage differential of 415 volts (E/N ~ 140 Td). The sample is mixed with the reagent ions in the FIMR and molecules with an ionization energy (I.E.) below that of oxygen (12.1 eV) ionize to produce predominantly M^+ ions (Linstrom and Mallard). Ions then travel to the coupled TOF mass analyzer with a nominal resolving power of 5000. This ionization method allows for the sensitive detection of species that do not form MH^+ ions via H_3O^+ chemistry, such as CS_2 and OCS.

The Vocus can be operated either as an *in situ* instrument for continuous, real-time measurements at high sample rates (RT-Vocus) or can be coupled to a gas chromatography (GC) system equipped with sample preconcentration (GC-Vocus) for more sensitive, molecular specific information (Kilgour et al., 2024). In the laboratory studies presented here, we use real-time O_2^+ CI-ToFMS to

https://doi.org/10.5194/egusphere-2026-5120
Preprint. Discussion started: 24 September 2026

determine the sensitivity (including its dependence on absolute humidity) and fragmentation patterns for the detection of CS_2, OCS, and DMS. Additionally, measurements from the Aerosol Growth in the Eastern North Atlantic (AGENA), the Summertime Measurements Of Key Illinois-Emitted Volatile Organic Compounds (SMOKIEVOC), and the Probing Ecosystem Response Involving Notable Organics (PEcoRINO) field campaigns were reanalyzed. During AGENA, the Vocus PTR-ToF-MS was deployed at the Atmospheric Radiation Measurement Facility on Graciosa Island, Azores, Portugal (39.0916° N, 28.0257° W; 30 m elevation) from 1 June to 15 July 2022 at 10 m above ground level. This paper utilizes the GC-Vocus data (Kilgour et al., 2024). During SMOKIEVOC, the Vocus was deployed in downtown Chicago at the University of Illinois Science and Engineering South building (845 West Taylor Street, Chicago IL 60607) from 15 July to 21 August 2023. This paper presents both the RT and GC-Vocus data (Rogers and Bertram, 2025). During PEcoRINO, the Vocus was deployed over the Chequamegon-Nicolet National Forest in Park Falls, WI (45.945◦ N, 90.273◦ W) from 6 to 30 September 2020 at 30 m above ground level. This paper utilizes the GC-Vocus data (Vermeuel et al., 2023). In all cases, the Vocus was operated using H_3O^+ reagent ions, but background O_2^+ ions permitted us to explore detection of CS_2 and OCS.

2.2 Calibration Procedures

The Vocus mass spectrometer, utilizing O_2^+ ion chemistry, was calibrated for CS_2, OCS, and DMS by delivering known concentrations of each molecule to the instrument inlet. Calibration gas mixtures were made using certified, standard compressed gas cylinders of CS_2, OCS, and DMS in N_2 (4.993 ppm CS_2, Airgas; 4.668 ppm OCS, Airgas; 5.08 ppm DMS, Praxair) mixed with UHP zero air (Airgas). Calibrations for CS_2 and OCS were conducted over a dynamic mixing ratio range of 0 - 6 ppb and for DMS over a range of 0 - 3ppb.

To assess the dependence of the sensitivity on absolute humidity, we humidified a fraction of the zero air flow by bubbling it through a water reservoir containing high purity water (Milli-Q, 18.2 MΩ·cm). The saturated air was mixed with a variable dry zero air to produce a wide range of relative humidity (3% - 63%). The relative humidity (RH) of the carrier flow gas was measured with an RH probe (Vaisala HMP110) placed behind the Vocus sampling inlet. Values were converted to absolute humidity (AH) for discussion.

3. Results and Discussion

3.1 Detection of carbon disulfide (CS_2)

M^+ product ions are formed in the charge transfer reaction with O_2^+ if the analyte ionization energy (I.E.) is smaller than that of O_2 (12.1 eV; see Linstrom and Mallard). In the case of CS_2 (I.E. = 10.1 eV; see Linstrom and Mallard), we expect to observe product ions as CS_2^+ (75.94 m/Q, Reaction 1). Likewise, proton transfer reaction products (MH^+) are formed in the reaction with H_3O^+ reagent ions when the proton affinity (P.A.) of the analyte is larger than that of H_2O (697 kJ mol^{-1}; see Krechmer et al., 2018) For CS_2 (P.A. = 682 kJ mol^{-1}; see Linstrom and Mallard), we do not expect

https://doi.org/10.5194/egusphere-2026-5120
Preprint. Discussion started: 24 September 2026

to measure the proton transfer product (CS_2H^+) under PTR ionization conditions and would not expect to observe a measurable CS_2H^+ product ion from residual H_3O^+ in the O_2^+ ionization condition (Reaction 2).

$$CS_2 + O_2^+ \rightarrow CS_2^+ + O_2 \quad \text{R1}$$

$$CS_2 + H_3O^+ \rightarrow CS_2H^+ + H_2O \quad \text{R2}$$

As expected in O_2^+ CI-ToFMS, the dominant ionization product (CS_2^+) is observed at 75.94 m/Q (**Fig. 1**). We observed the following product ions, where the exact mass of the product ion and the fractional contribution to the total CS_2 product ion distribution are included in paratheses: CS_2^+ (75.94 m/Q, 0.983), CS_2O^+ (91.93 m/Q, 0.008), OCS^+ (59.97 m/Q, 0.005), and S_2^+ (63.94 m/Q, 0.004). We also observe the isotopologues $CS^{34}S^+$ (77.94 m/Q), $C^{34}S_2^+$ (79.97 m/Q), and $^{13}CS_2^+$ and $CS^{33}S^+$ (76.94 m/Q). All isotopes were measured at the expected fractional contributions based on their natural abundances of 0.090, 0.002, and 0.027 respectively.

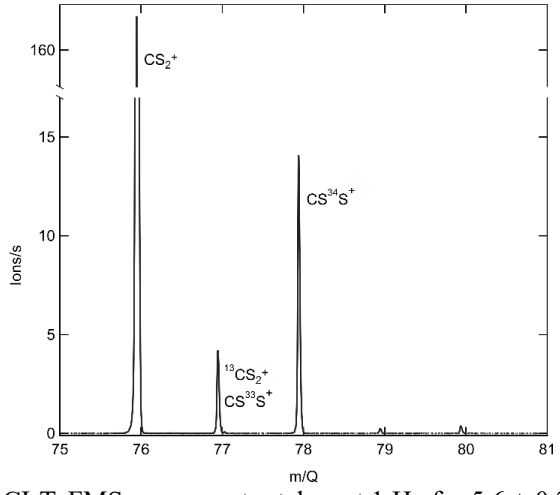

Figure 1. Sample O_2^+ CI-ToFMS mass spectra taken at 1 Hz for 5.6 ± 0.28 ppb CS_2 in ultra-pure zero air. The dominant product ion peak is CS_2^+ (75.94 m/Q). Additional product ions include CS_2O^+ (91.93 m/Q, 0.008), OCS^+ (59.97 m/Q, 0.005), and S_2^+ (63.94 m/Q, 0.004). Observed isotopologues include $^{13}CS_2^+$ and $CS^{33}S^+$ (76.95 m/Q) and $CS^{34}S^+$ (77.94 m/Q).

To assess the contribution of ions with the same nominal mass to charge ratio as CS_2^+ (75.94 m/Q) under O_2^+ ionization conditions, we conducted a short experiment in which we sampled ambient urban air in Madison, WI. A typical ambient mass spectrum centered at 76 m/Q is shown in **Fig. 2**. Ions contributing to the total ion count rate at 76 m/Q include: $C_2H_4OS^+$ (76.00 m/Q), $C_2H_4O_3^+$ (76.02 m/Q), $C_3H_8O_2^+$ (76.05 m/Q), $C_2{}^{13}CH_7O_2^+$ (76.05 m/Q), and $C_3H_6O^{18}O^+$ (76.04 m/Q). In this environment, CS_2^+ contributes more than 35% of the total ion current at 76 m/Q and is 0.5 amu from the next nearest contributing ion ($C_2H_4OS^+$). Additionally, it is reasonably resolved with

https://doi.org/10.5194/egusphere-2026-5120
Preprint. Discussion started: 24 September 2026

our instrument resolving power of 5000 highlighting that a moderately high-resolution mass analyzer is required for isolation of the CS_2^+ ion.

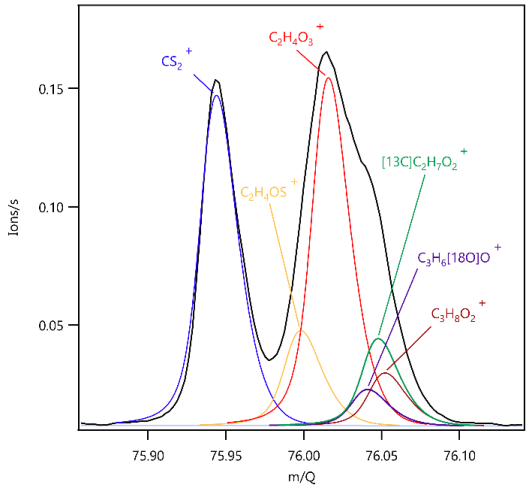

Figure 2. Ambient O_2^+ CI-ToFMS mass spectra taken at 1 Hz and centered at 76 m/Q collected in Madison, WI in November 2024. Ions contributing to the total count rate at 76 m/Q include CS_2^+ (75.94 m/Q, carbon disulfide), $C_2H_4OS^+$ (76.00 m/Q), $C_2H_4O_3^+$ (76.02 m/Q), $C_3H_8O_2^+$ (76.05 m/Q), $C_2{}^{13}CH_7O_2^+$ (76.05 m/Q), and $C_3H_6O^{18}O^+$ (76.04 m/Q). Black trace represents the measured signal. Colored traces show assigned fits.

The sensitivity of the CS_2^+ product ion was determined to be 0.092 cps ppt^{-1} for the concentration range of 0 - 6000 ppt under O_2^+ ionization conditions (**Fig. 3a**). The calibration is linear over this concentration range ($R^2 = 1$). The background count rate for CS_2^+ in zero air was determined to be 0.15 ± 0.09 cps (1σ, 10 s average). For these conditions, we derive a 10-second, 3σ average limit of detection of 12 ppt. To place the sensitivity in context, we also measured the sensitivity of the O_2^+ CI-ToFMS to benzene ($C_6H_6^+$, 0.15 cps ppt^{-1}) and acrylonitrile ($C_3H_3N^+$, 0.11 cps ppt^{-1}). The dominant product ion for both benzene and acrylonitrile was the M^+ charge transfer ion, indicating minimal fragmentation of the primary M^+ product ion (Linstrom and Mallard). The reported sensitivities for all three molecules represent a lower limit for this type of Vocus mass spectrometer, as the experiments reported here were conducted with an aging detector and discharge electrodes. Utilizing acetone as a well characterized instrument sensitivity tracer, we expect a sevenfold increase in our reported CS_2 sensitivity (up to 0.7 cps ppt^{-1}) under optimal conditions (0.77 cps ppt^{-1} in this study compared to 5.6 cps ppt^{-1} when the instrument is running in an optimal configuration).

https://doi.org/10.5194/egusphere-2026-5120
Preprint. Discussion started: 24 September 2026

In our PTR-MS configuration, we do not observe a sensitivity dependence on the humidity of the sampled air because the H_3O^+ reagent ion saturates the ionization region (Krechmer et al., 2018), but this is not the case for O_2^+ CI-ToFMS. To determine the impact of humidity on the sensitivity of CS_2^+, we measured the instrument sensitivity as a function of the absolute humidity between 0-15 g m^{-3}, where the nominally dry case corresponded to an absolute humidity of 0.53 ± 0.10 g m^{-3}. This is within the range of absolute humidities observed in the Azores (2.2 – 17.8 g m^{-3}) and Chicago (7.8 – 23.3 g m^{-3}) during their respective campaigns. As shown in **Fig. 3b**, CS_2^+ displays a weak dependence on absolute humidity, with a percentage change in sensitivity of less than 10% compared to dry conditions. The slight variations observed are likely due to the formation of $O_2(H_2O)^+$ clusters. The ratio of O_2^+ to $O_2(H_2O)$ may shift with absolute humidity affecting our sensitivity.

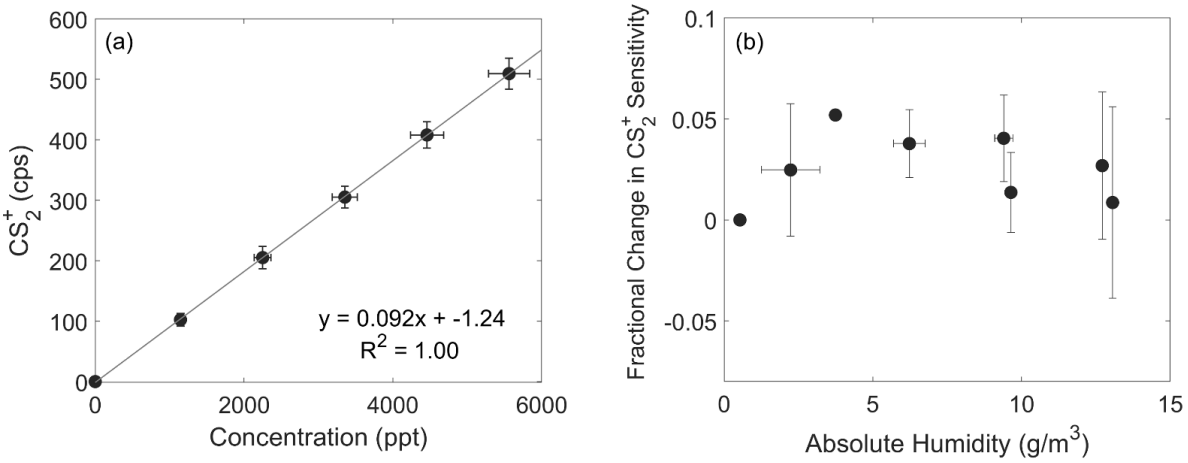

Figure 3. (a) O_2^+ CI-ToFMS calibration to CS_2^+ in the 0 - 6 ppb range. The sensitivity is 0.092 cps ppt^{-1} (R^2 = 0.99997) with a background count rate of 0.15 ± 0.09 cps (1s, 10 s avg) and LOD of 12 ppt (3s, 10 s avg). Error bars represent standard deviation of signal averaging and error in CS_2 concentration. The standard errors of the slope and *y*-intercept are 2.5×10^{-4} and 0.86 respectively. Calibrations repeated in triplicates. **(b)** The fractional change in CS_2^+ sensitivity as a function of absolute humidity at 5.0 ± 0.18 ppb CS_2. Error bars represent uncertainty in sensitivity and standard deviation of RH probe output averaging.

3.2 Detection of carbonyl sulfide (OCS)

For OCS (I.E. = 11.2 eV; see Linstrom and Mallard), we expect to observe O_2^+ ionization product ions as OCS^+ (59.97 m/Q, Reaction 3). Similarly to CS_2, we do not expect protonation of OCS to occur (P.A. = 628.5 kJ/mol; see Linstrom and Mallard) under PTR or O_2^+ ionization conditions as the reaction is unfavorable (Reaction 4).

$$OCS + O_2^+ \rightarrow OCS^+ + O_2 \quad \text{(R3)}$$

$$OCS + H_3O^+ \rightarrow OCSH^+ + H_2O \quad \text{(R4)}$$

https://doi.org/10.5194/egusphere-2026-5120
Preprint. Discussion started: 24 September 2026

The only product ion measured in O_2^+ CI-ToFMS is OCS^+ at 59.97 m/Q. No other major product ions or fragments of OCS are detected, but the isotopologues $OC^{34}S^+$ (61.96 m/Q) and $OC^{33}S^+$ and $O^{13}CS$ (60.97 m/Q) are observed at the expected fractional contributions based on their natural abundances of 0.042 and 0.018 respectively (**Fig. 4**).

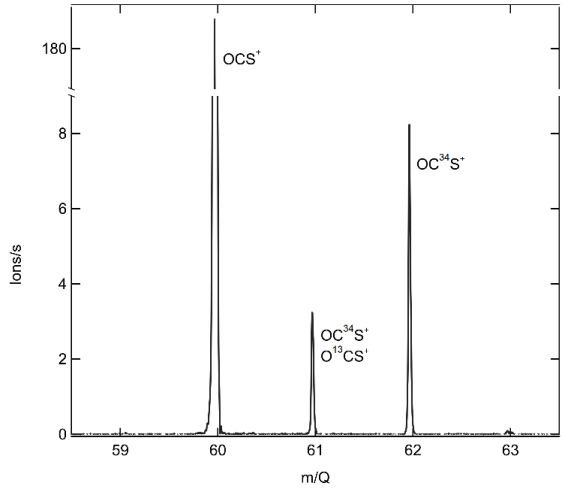

Figure 4. O_2^+ CI-ToFMS mass spectra taken at 1 Hz of 5.2 ± 0.26 ppb OCS in ultra-pure zero air. The dominant product ion peak is OCS^+ (59.97 m/Q). Isotopologues observed include $OC^{34}S^+$ (61.96 m/Q) and $OC^{33}S^+$ and $O^{13}CS$ (60.97 m/Q).

A typical O_2^+ CI-ToFMS ambient mass spectrum centered at 60 m/Q is shown in **Fig. 5** to assess the contribution of ions with the same nominal mass to charge ratio as OCS^+. Ions contributing to the total ion count rate at 60 m/Q include: $C_2H_4O_2^+$ (60.02 m/Q), $C_3H_8O^+$ (60.06 m/Q), and $C_2{}^{13}CH_7O^+$ (60.05 m/Q). For the ambient urban measurements conducted in Madison, WI, OCS^+ was found to contribute approximately 60% of the total ion current and is 0.05 amu from the nearest contributing ion ($C_2H_4O_2^+$). Similarly, it is reasonably resolved with our resolving power of 5000 indicating the need for a moderately high-resolution mass analyzer for isolation of the OCS^+ ion.

https://doi.org/10.5194/egusphere-2026-5120
Preprint. Discussion started: 24 September 2026

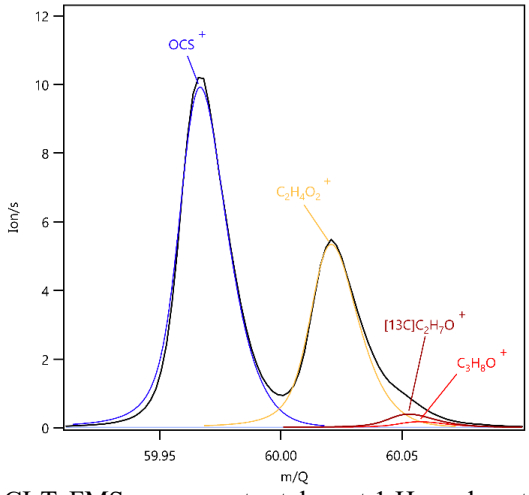

Figure 5. Ambient O_2^+ CI-ToFMS mass spectra taken at 1 Hz and centered at 60 m/Q. Collected in Madison, WI in November 2024. Ions contributing to the total count rate are: OCS^+ (59.97 m/Q, carbonyl sulfide), $C_2H_4O_2^+$ (60.02 m/Q), $C_3H_8O^+$ (60.06 m/Q), and $C_2{}^{13}CH_7O^+$ (60.05 m/Q). Black trace represents the measured signal. Colored traces show assigned fits.

The OCS sensitivity as measured with the OCS^+ product ion was determined to be 0.10 cps ppt^{-1} for the concentration range of 0 - 6000 ppt under O_2^+ ionization conditions (**Fig. 6a**). The calibration is linear over this concentration range ($R^2 = 1$). The background count rate for OCS^+ in zero air was found to be 0.84 ± 0.26 cps (1σ, 10 s avg). A 10-second, 3σ average limit of detection of 17 ppt (3σ, 10 s avg) was derived under these conditions. With a similar sensitivity to CS_2^+, we again suspect minimal fragmentation of the primary M^+ product ion. As discussed above, we expect a sevenfold increase in our reported OCS sensitivity (up to 0.7 cps ppt^{-1}) when the instrument is running in an optimal configuration.

Instrument sensitivity as a function of the absolute humidity between 0-15 g m^{-3}, where the nominally dry case corresponds to an absolute humidity of 0.54 ± 0.11 g/m^3, was measured to determine the impact of humidity on the sensitivity of OCS^+. OCS^+ displays a stronger dependence on absolute humidity in comparison to CS_2^+, with a percent decrease in sensitivity of around 20% compared to dry conditions. This humidity dependence can be attributed to the formation of $OCS(H_2O)^+$ clusters. When accounting for $OCS(H_2O)^+$ clusters, change in OCS sensitivity reduces to less than 5% compared to dry conditions (**Fig. 6b**).

https://doi.org/10.5194/egusphere-2026-5120
Preprint. Discussion started: 24 September 2026

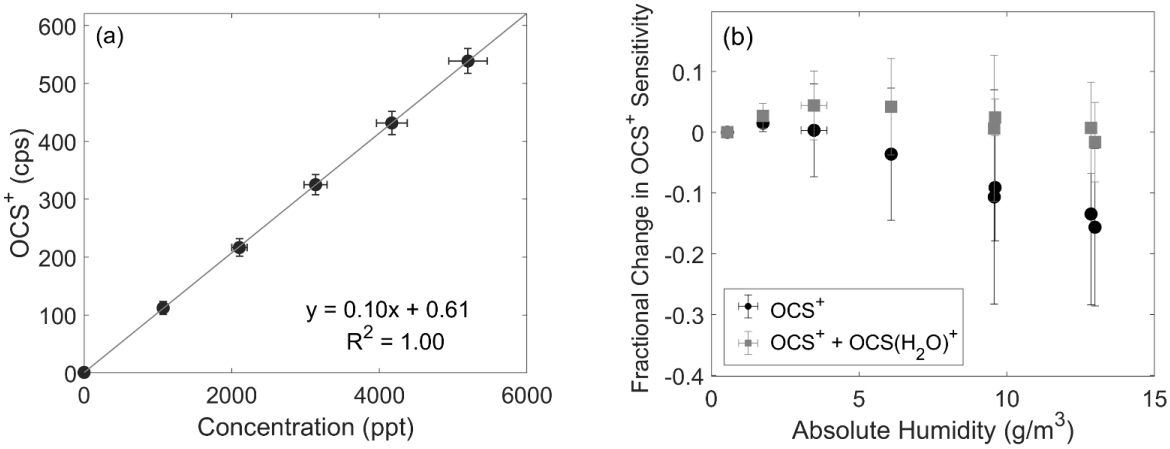

Figure 6. (a) O_2^+ CI-ToFMS calibration to OCS^+ in the 0 - 6 ppb range. The sensitivity is 0.10 cps ppt^{-1} (R^2 = 0.99998) with a background count rate of 0.84 ± 0.26 cps (1s, 10 s avg) and LOD of 17 ppt (3s, 10 s avg). Error bars represent standard deviation of signal averaging and error in OCS concentration. The standard errors of the slope and *y*-intercept are 2.1 × 10^{-4} and 0.67 respectively. Calibrations repeated in triplicate. **(b)** The fractional change in OCS^+ and OCS^+ + $OCS(H_2O)^+$ sensitivity as a function of absolute humidity at 4.6 ± 0.17 ppb OCS. Error bars represent uncertainty in sensitivity and standard deviation of RH probe output averaging.

3.3 Detection of dimethyl sulfide (C_2H_6S, DMS)

When considering DMS (I.E = 8.7 eV; see Linstrom and Mallard), we expect to observe the O_2^+ ionization product ion as $C_2H_6S^+$ (62.02 m/Q, Reaction 5). However, unlike CS_2 and OCS, we also expect to observe the proton transfer product ($C_2H_6SH^+$, 63.03 m/Q) as this reaction is favorable for DMS (P.A. = 830.9 kJ/mol, Reaction 6; see Linstrom and Mallard). Due to its high proton affinity, we expect to see measurable $C_2H_6SH^+$ product ion under both PTR ionization conditions and from residual H_3O^+ in the O_2^+ ionization conditions.

$$C_2H_6S + O_2^+ \rightarrow C_2H_6S^+ + O_2 \quad \text{(R5)}$$

$$C_2H_6S + H_3O^+ \rightarrow C_2H_6SH^+ + H_2O \quad \text{(R6)}$$

As expected, the primary O_2^+ ionization product, $C_2H_6S^+$, is present at 62.02 m/z, however, it contributes to less than half of the total DMS signal. Due to the low bond energy of its C-S bond, the DMS mass spectrum contains many high intensity fragments and product ions including: CH_3SO^+ (62.99 m/z), $CH_3SO_2^+$ (78.98 m/z), $C_2H_6SO^+$ (78.01 m/Q), and $C_2H_5O^+$ (61.01 m/Q). When considering existing data and the analysis of isotopically labeled DMS ($C_2H_3[2H]_3S$, d3-DMS), we also expect the formation of fragment ions CH_3S^+ (46.99 m/Q), CH_2S^+ (45.99 m/Q), and CHS^+ (44.98 m/Q), however they could not be properly assigned due to interference with a very large NO_2^+ peak (45.99 m/Q). Additionally, we observe the isotopologues $C_2H_6{}^{34}S^+$ (64.01 m/Q) at a fractional contribution slightly lower than expected based on its natural abundance

https://doi.org/10.5194/egusphere-2026-5120
Preprint. Discussion started: 24 September 2026

(0.042) likely due to the high degree of fragmentation observed (**Fig. 7**). The proton transfer product, $C_2H_6SH^+$ (63.03 m/Q), is not observed as H_3O^+ is nearly absent in dry, laboratory

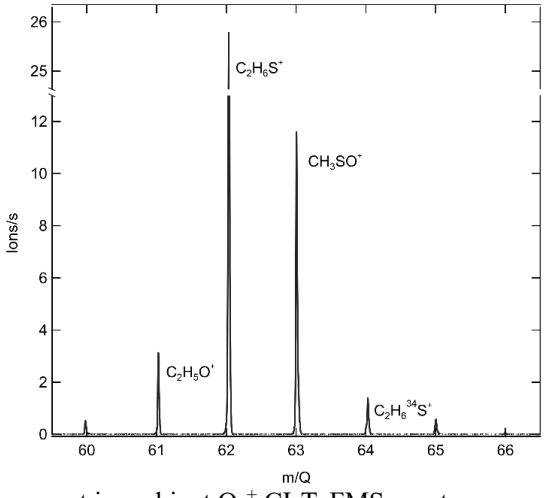

conditions, though it is present in ambient O_2^+ CI-ToFMS spectra.

Figure 7. O_2^+ CI-ToFMS mass spectra taken at 1 Hz of 2.7 ± 0.14 ppb DMS in ultra-pure zero air. The dominant product ion peak is $C_2H_6S^+$ (62.02 m/Q). Additional product ions include: CH_3SO^+ (62.99 m/z), $CH_3SO_2^+$ (78.98 m/z), $C_2H_6SO^+$ (78.01 m/Q), $C_2H_5O^+$ (61.01 m/Q), and $C_2H_6{}^{34}S^+$ (64.01 m/Q).

A typical ambient spectrum centered at 62 m/Q is shown in **Fig. 8**. A short experiment was conducted in Madison, WI to assess the contribution of ions with the same nominal mass to charge ratio as the $C_2H_6S^+$ ion. Ions contributing to the total ion count rate at 62 m/Q include: $OC^{34}S^+$ (61.96 m/Q), $C_2H_3Cl^+$ (61.99 m/Q), $C_2H_6O_2^+$ (62.04 m/Q), $C_2H_4O^{18}O^+$ (62.02 m/Q) and $C^{13}CH_5O_2^+$ (62.03 m/Q). In these conditions, $C_2H_6S^+$ contributes less than 20% of the total ion current and is only 0.01 amu from the nearest contributing ion ($C_2H_4O^{18}O^+$). It is not well resolved with our resolving power of 5000, highlighting that a high-resolution mass analyzer is required for isolation of the $C_2H_6S^+$ ion. In settings with higher DMS concentrations, like marine environments, we would expect the $C_2H_6S^+$ ion to be present in a larger proportion.

https://doi.org/10.5194/egusphere-2026-5120
Preprint. Discussion started: 24 September 2026

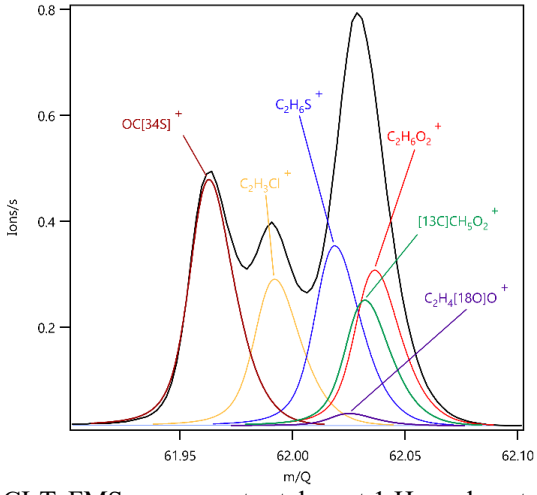

Figure 8. Ambient O_2^+ CI-ToFMS mass spectra taken at 1 Hz and centered at 62 m/Q. Collected in Madison, WI in November 2024. Ions contributing to the total count rate are: $OC^{34}S^+$ (61.96 m/Q), $C_2H_3Cl^+$ (61.99 m/Q), $C_2H_6O_2^+$ (62.04 m/Q), $C_2H_4O^{18}O^+$ (62.02 m/Q) and $C^{13}CH_5O_2^+$ (62.03 m/Q). Black trace represents the measured signal. Colored traces show assigned fits.

The sensitivity of the $C_2H_6S^+$ product ion was observed to be 0.027 cps ppt^{-1} for the concentration range of 0 - 3000 ppt (**Fig. 9**). This calibration is linear over this concentration range ($R^2 = 1$). The background count rate for $C_2H_6S^+$ in zero air was determined to be 0.11 ± 0.11 cps (1σ, 10 s average) and a 10-second, 3σ average limit of detection was derived to be 46 ppt under these conditions. This sensitivity is approximately five times smaller than that observed for CS_2^+ and OCS^+. To place this in context, we compare it to the measured O_2^+ CI-ToFMS sensitivity of isoprene ($C_5H_8^+$, 0.027 cps ppt^{-1}) and trimethylbenzene ($C_9H_{12}^+$, 0.033 cps ppt^{-1}). While the M^+ charge transfer ion was the dominant ion product for isoprene, it accounted for less than 20% of the total signal. The M^+ ion of trimethylbenzene also accounted for around 20% of the total signal, however, it was not the dominant ion (Linstrom and Mallard). This indicates a high degree of fragmentation and aligns with the large fragmentation discussed above. The reported sensitivity again represents a lower limit with potential for a sevenfold increase under optimal instrument conditions, however even with this O_2^+ CI-ToFMS looks to be inferior to PTR-MS for the detection of DMS (0.29 cps ppt^{-1}). Instrument sensitivity of DMS as a function of absolute humidity was not explored.

https://doi.org/10.5194/egusphere-2026-5120
Preprint. Discussion started: 24 September 2026

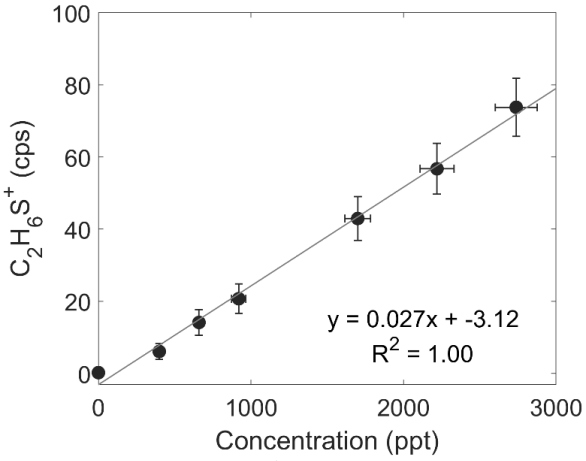

Figure 9. O_2^+ CI-ToFMS calibration to $C_2H_6S^+$ in the 0 - 3 ppb range. The sensitivity is 0.027 cps ppt^{-1} (R^2 = 0.995) with a background count rate of 0.11 ± 0.11 cps (1σ, 10 s average) and LOD of 46 ppt (3σ, 10 s avg). Error bars represent standard deviation of signal averaging and error in DMS concentration. The standard errors of the slope and *y*-intercept are 8.3×10^{-4} and 1.3 respectively.

3.4 Field Measurements of Carbon Disulfide (CS_2)

Here, we report on the reanalysis of mass spectra collected in three prior field campaigns, where the Vocus was operated using H_3O^+ chemistry, but residual O_2^+ provides an opportunity to measure CS_2. While in retrospect, it would have been far more advantageous to have operated the instrument in a deliberate O_2^+ sampling configuration, we think that the observations are still a valuable contribution due to the extreme paucity of CS_2 measurements in the literature. Other existing datasets collected under PTR ionization conditions may also utilize the method below to quantify CS_2 via secondary O_2^+ ionization chemistry in an effort to add to the very sparse collection of gas-phase CS_2 measurements.

CS_2 was detected as the M^+ product ion (CS_2^+) in the AGENA (Graciosa Island, Azores) and SMOKIEVOC (Chicago, IL) field campaigns. In both studies, CS_2 was almost exclusively observed in the GC-Vocus measurement as preconcentration was required to measure the trace quantities given the instrument's low sensitivity when operating in PTR mode. Representative GC chromatograms are shown in **Fig. 10**, where the M^+ product ions of CS_2 (CS_2^+) and DMS ($C_2H_6S^+$), formed via residual O_2^+, are separated by their unique mass to charge, but also their retention time on the GC column. DMS elutes near CS_2 in the GC as expected based on their respective Kovat retention indices of 516 and 563 (Linstrom and Mallard). This is confirmed through laboratory measurements with certified standards. Chromatograms are background subtracted (**Fig. S1 and S2**) and no other peaks are observed besides the M^+ product ions (**Fig. S3**). DMS was not observed in the chromatograms taken in Chicago.

https://doi.org/10.5194/egusphere-2026-5120
Preprint. Discussion started: 24 September 2026

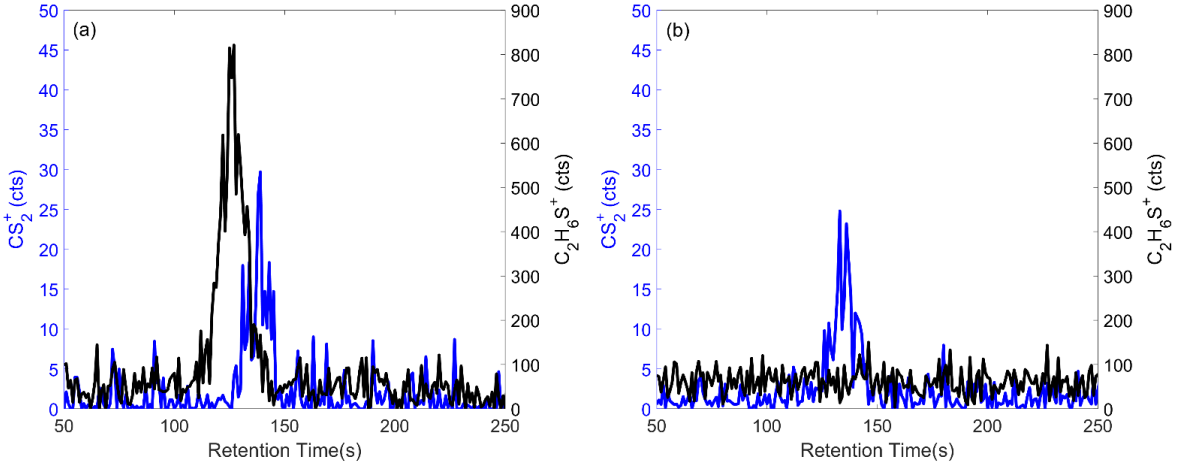

Figure 10. Representative CS_2^+ (blue) and $C_2H_6S^+$ (black) chromatograms taken at 5 Hz (1-second average) for **(a)** AGENA (Graciosa Island, Azores) and **(b)** SMOKIEVOC (Chicago, IL) field campaigns. Trapping volumes are 3 L and 0.5 L respectively.

To calibrate the measured CS_2^+ signal during the field campaigns, we scaled our continuous in-field PTR measurements of d3-DMS^+ ($C_2H_3[2H]_3S^+$, 65 m/z) sensitivity ($S_{d3-DMS^+,field}$) by the ratio of our laboratory PTR measurements of CS_2^+ ($S_{CS_2^+,lab}$) and DMS^+ sensitivity ($S_{DMS^+,lab}$) to determine the appropriate in-field sensitivity to CS_2^+($S_{CS_2^+,field}$), as described in **Eq. (1).**

$$S_{CS_2^+,field} = S_{d3-DMS^+,field} \times \frac{S_{CS_2^+,lab}}{S_{DMS^+,lab}} \quad (1)$$

In AGENA, d3-DMS was continuously added to the sampling inlet as a standard addition so that instrument sensitivity could be tracked continuously. DMS was chosen as a representative laboratory calibrant as both it and d3-DMS undergo a comparable charge transfer reaction with O_2^+ ionization as they exhibit the same ionization energy of 8.7 eV (Linstrom and Mallard). For the Chicago measurements, a 14-molecule VOC standard was used for daily calibration. Since DMS was not part of the calibration mixture, benzene was chosen as the transfer standard for the Chicago measurements, due to its high charge transfer efficiency (I.E. = 9.2; see Linstrom and Mallard) with O_2^+ and thus large presence of its M^+ product ion. For the Chicago measurements, **Eq. (1)** is modified to include benzene sensitivities in place of the d3-DMS sensitivities.

From 5-step triplicate calibration measurements in the concentration range of 0 - 7 ppb, the RT-Vocus sensitivities of the M^+ product ion under PTR ionization conditions were 0.026 cps ppt^{-1}, 0.012 cps ppt^{-1}, and 0.032 cps ppt^{-1} for CS_2, DMS, and benzene respectively (R^2 = 0.99). This resulted in a $CS_2^+/C_2H_6S^+$ laboratory sensitivity ratio of 2.1 and a $CS_2^+/C_6H_6^+$ laboratory sensitivity ratio of 0.81. Strong signal correlation (R^2 > 0.96) of the charge transfer product ion (M^+) and

https://doi.org/10.5194/egusphere-2026-5120
Preprint. Discussion started: 24 September 2026

proton transfer ion (MH^+) across both campaigns proves this quantification method to be reliable and robust (**Fig. S4**).

In the Azores, CS_2 was detected consistently across the campaign with more than 85% (95/110) of GC-Vocus measurements having a detectable CS_2 peak in the GC chromatogram that could be fit. Peaks were generally considered to be unresolvable when the peak intensity was less than 1.5× the signal intensity of the surrounding noise. A distribution of the measurements is shown in **Fig. 11a**. The mean concentration of CS_2 is between 1.9 (± 1.6) ppt and 2.5 (± 1.7) ppt as defined by the treatment of the unresolved GC measurements. The limits represent when the unresolved peaks are equated to 0 ppt and the limit of detection (LOD, 2.0 ppt) respectively. When treated as 0.5× the LOD, the mean CS_2 concentration is 2.2 (± 1.4) ppt. This data is on the lower range of previously reported gas-phase marine boundary layer concentrations (2.5 to 275.7 ppt) highlighting the need for more quantitative measurements to discern global spatial patterns of CS_2 (Lennartz et al., 2020). These mean concentrations of CS_2 are significantly lower than other marine sulfur species, DMS (107 ± 69 ppt) and MeSH (15 ± 12 ppt), observed in the Azores (Kilgour et al., 2025). No trends between CS_2 and DMS or MeSH are seen and the little variability observed in CS_2 is consistent with a diffuse, continuous source such as the ocean.

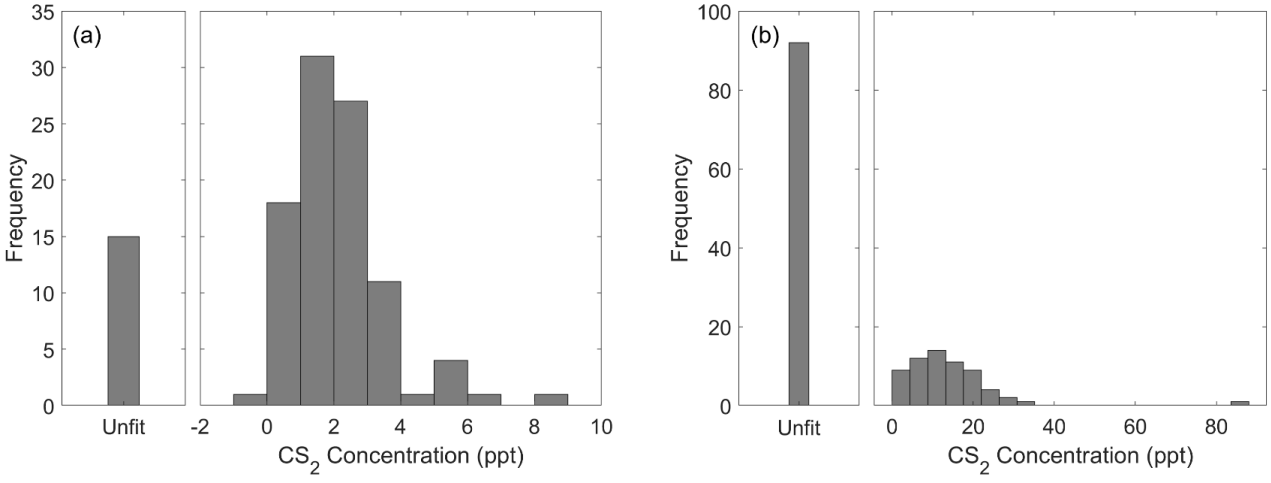

Figure 11. Histogram of CS_2 concentration (ppt) in **(a)** AGENA (Graciosa Island, Azores) and **(b)** SMOKIEVOC (Chicago, IL) from GC-Vocus measurements. The unfit region represents measurements with no resolvable CS_2^+ peak in the GC chromatogram.

In Chicago, CS_2 was far more variable and detected less consistently with only 40% (63/155) of GC-Vocus measurements containing detectable CS_2. The mean CS_2 concentration ranges from 5.6 (± 10.1) ppt to 13 (± 7.6) ppt when considering unresolvable GC measurements as 0 ppt and the LOD (13 ppt), respectively, highlighting the high variability of this site. When unresolved peaks were replaced with 0.5× the LOD, the mean concentration was 9.5 (± 8.3) ppt, significantly larger than the CS_2 concentration observed in AGENA. Notably, we measured an anomalously CS_2-rich airmass in Chicago where the CS_2 concentration peaked at 87 ppt. This is displayed via histogram

https://doi.org/10.5194/egusphere-2026-5120
Preprint. Discussion started: 24 September 2026

in **Fig. 11b**. This data is consistent with other urban measurements reported from the TRACE-P aircraft campaign. Plumes of polluted, urban air transported from northern China were observed near the coast where individual measurements of CS_2 peaked at 90 ppt (Blake et al., 2004). The large CS_2 enhancement present in Chicago GC-Vocus can also be seen in the RT-Vocus measurements. The 5-minute averaged RT-Vocus CS_2 time series is shown in **Fig. 12** overlayed with the GC-Vocus measurements. The source of this CS_2 enhancement is currently unknown, but wind data shows that a large portion of RT-Vocus CS_2^+ signal detected 2 standard deviations above the mean originates from the south direction. This is displayed via wind rose in **Fig. 13a**. A satellite image of the sampling location and surrounding area is shown in **Fig. 13b**, but since CS_2 has an atmospheric lifetime of a few days, source identification is challenging. We did not observe another ion in the RT or GC-Vocus spectra that covaried with the CS_2 enhancement, suggesting that the emission rate of other molecules from this source is small relative to their respective background concentrations in the polluted Chicago airmass.

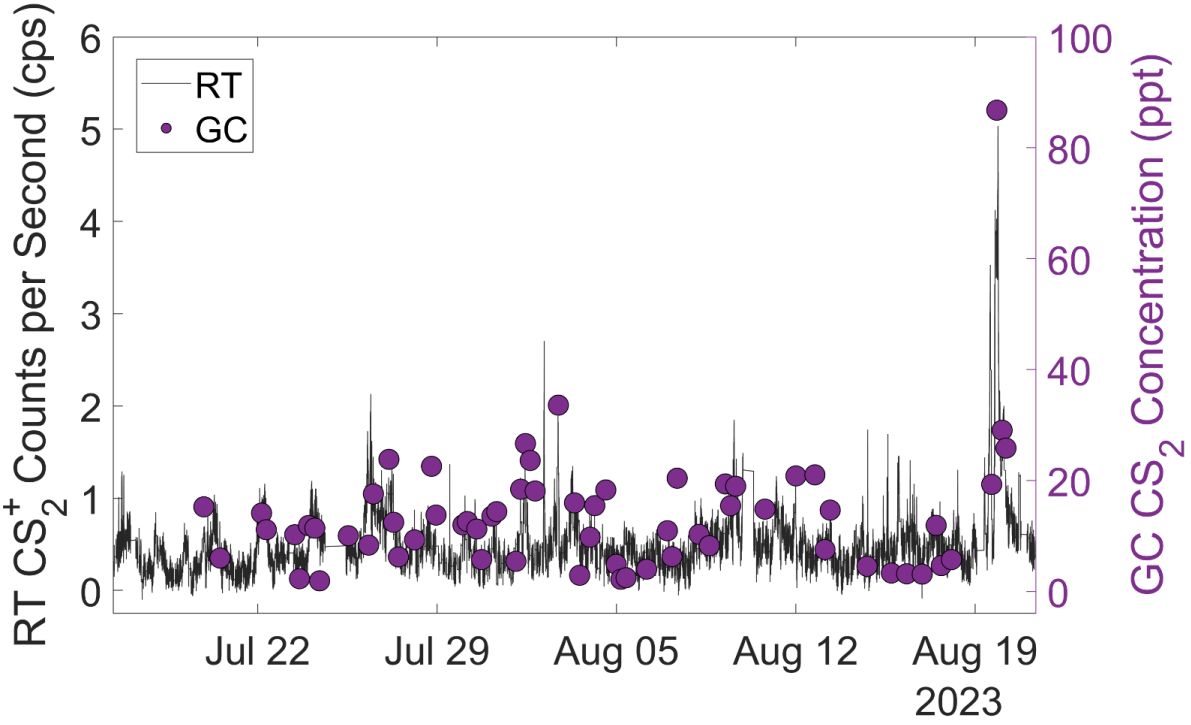

Figure 12. Gas chromatography (GC, purple) and 5-minute moving averaged real time (RT, black)-Vocus measurements of CS_2 from the SMOKIEVOC (Chicago, IL) campaign.

https://doi.org/10.5194/egusphere-2026-5120
Preprint. Discussion started: 24 September 2026

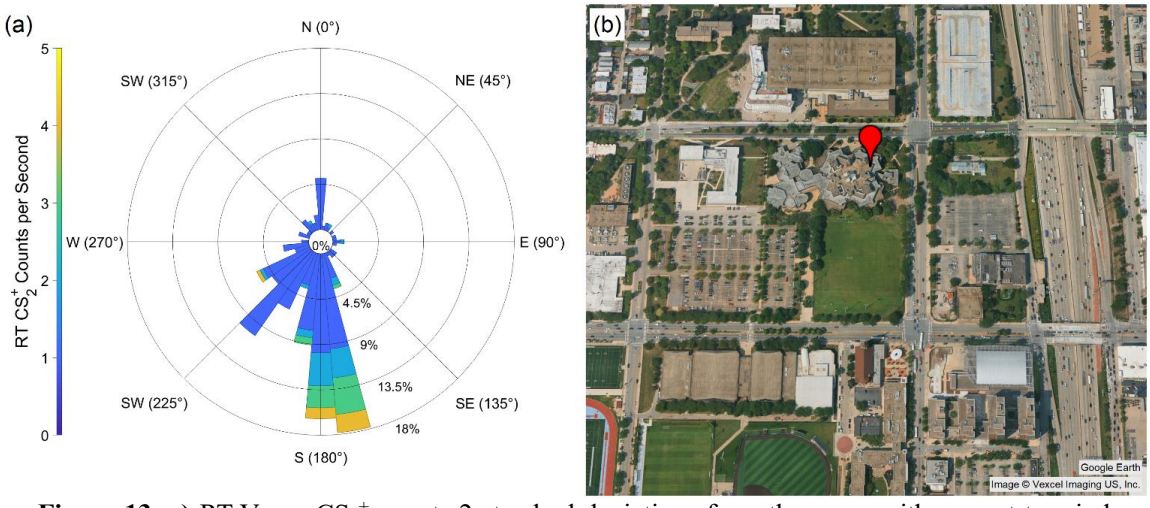

Figure 13. a) RT-Vocus CS_2^+ counts 2 standard deviations from the mean with respect to wind direction across the SMOKIEVOC (Chicago, IL) campaign and **b)** a satellite image of the sampling site (red marker) and the surrounding area.

Finally, we reanalyzed a GC Vocus dataset from Northern Wisconsin (PEcoRINO; see Vermeuel et al., 2023). In this analysis, less than 10% of GC-Vocus measurements display detectable CS_2^+ peaks that are 1.5× the surrounding noise. This was expected as the campaign was completed over a remote mixed temperate forest in Northern Wisconsin, far from large marine or anthropogenic sources.

4. Conclusion

We show that use of O_2^+ CI-ToFMS provides reliable, atmospherically relevant detection and quantification of the sulfur trace gases CS_2 and OCS. We demonstrate that CS_2 is detected primarily as CS_2^+ with less than 2% signal abundance attributed to fragments. OCS is detected solely as OCS^+. DMS is detected primarily as $C_2H_6S^+$, but much of its signal is spread through a series of fragment ions (>58%), making O_2^+ ion chemistry less well suited for ambient measurements of DMS when compared with H_3O^+. All species of interest were reasonably resolvable from potential interfering peaks when using a mass analyzer with a nominal resolving power of 5000. Utilizing M^+ product ion sensitivity ratios under PTR conditions, we determined mean CS_2 mixing ratios of 2.2 ppt and 9.5 ppt for measurements taken at a remote marine surface site in the Eastern North Atlantic and Downtown Chicago, IL, respectively. CS_2 was not detected in Northen Wisconsin. In Chicago, we observed a large CS_2 signal enhancement indicative of unknown urban CS_2. Collectively, these results indicate the utility of O_2^+ ion chemistry as a primary and secondary ion source for simultaneous measurements of CS_2 and OCS that could be used to greatly expand the limited, current gas-phase database for CS_2 and better constrain global OCS budgets.

https://doi.org/10.5194/egusphere-2026-5120
Preprint. Discussion started: 24 September 2026

Data availability

CS_2 time series from the AGENA (GC-Vocus) and SMOKIEVOC (RT and GC-Vocus) field campaigns are available at https://digital.library.wisc.edu/1793/98044

Author contributions

ENK, DBK, and THB conceptualized the main ideas of the paper. DBK and CMJ collected GC-Vocus data in Graciosa Island, Azores. MNR collected RT and GC-Vocus data in Chicago, IL. MPV collected GC-Vocus data in Northern Wisconsin. ENK conducted and analyzed laboratory experiments, reanalyzed field data, and wrote the paper with input from THB. All authors reviewed and edited the paper.

Competing interests

The authors declare that they have no conflict of interest.

Financial Support

This material is based upon work supported by the US Department of Energy, Office of Science, Office of Biological and Environmental Research, Atmospheric System Research (ASR) (award no. DE-SC0021985). This research used resources of the Atmospheric Radiation Measurement (ARM) user facility, which is a DOE Office of Science user facility (award no. AFC010011).

References

Bandy, A. R., Maroulis, P. J., Bonsang, B., and Brown, C. A.: Emissions of Sulfur Gases to the Atmosphere from Estuaries and Coastal Areas, in: Estuarine Comparisons, edited by: Kennedy, V. S., Academic Press, 303–312, https://doi.org/10.1016/B978-0-12-404070-0.50024-7, 1982.

Blake, N. J., Streets, D. G., Woo, J.-H., Simpson, I. J., Green, J., Meinardi, S., Kita, K., Atlas, E., Fuelberg, H. E., Sachse, G., Avery, M. A., Vay, S. A., Talbot, R. W., Dibb, J. E., Bandy, A. R., Thornton, D. C., Rowland, F. S., and Blake, D. R.: Carbonyl sulfide and carbon disulfide: Large-scale distributions over the western Pacific and emissions from Asia during TRACE-P, J. Geophys. Res. Atmos., 109, https://doi.org/10.1029/2003JD004259, 2004.

Brühl, C., Lelieveld, J., Crutzen, P. J., and Tost, H.: The role of carbonyl sulphide as a source of stratospheric sulphate aerosol and its impact on climate, Atmos. Chem. Phys., 12, 1239–1253, https://doi.org/10.5194/acp-12-1239-2012, 2012.

Chin, M.: Atmospheric studies of carbonyl sulfide and carbon disulfide and their relationship to stratospheric background sulfur aerosol, Ph.D., Georgia Institute of Technology, United States -- Georgia, 181 pp., 1992.

Chin, M. and Davis, D. D.: Global sources and sinks of OCS and CS_2 and their distributions, Glob. Biogeochem. Cycles, 7, 321–337, https://doi.org/10.1029/93GB00568, 1993.

https://doi.org/10.5194/egusphere-2026-5120
Preprint. Discussion started: 24 September 2026

Cooper, D. J. and Saltzman, E. S.: Measurements of atmospheric dimethylsulfide, hydrogen sulfide,and carbon disulfide during GTE/CITE 3, J. Geophys. Res. Atmos., 98, 23397–23409, https://doi.org/10.1029/92JD00218, 1993.

Guo, H., Simpson, I. J., Ding, A. J., Wang, T., Saunders, S. M., Wang, T. J., Cheng, H. R., Barletta, B., Meinardi, S., Blake, D. R., and Rowland, F. S.: Carbonyl sulfide, dimethyl sulfide and carbon disulfide in the Pearl River Delta of southern China: Impact of anthropogenic and biogenic sources, Atmos. Environ., 44, 3805–3813, https://doi.org/10.1016/j.atmosenv.2010.06.040, 2010.

Jernigan, C. M., Fite, C. H., Vereecken, L., Berkelhammer, M. B., Rollins, A. W., Rickly, P. S., Novelli, A., Taraborrelli, D., Holmes, C. D., and Bertram, T. H.: Efficient Production of Carbonyl Sulfide in the Low-NO_x Oxidation of Dimethyl Sulfide, Geophys. Res. Lett., 49, e2021GL096838, https://doi.org/10.1029/2021GL096838, 2022.

Kilgour, D. B., Jernigan, C. M., Zhou, S., Brito de Azevedo, E., Wang, J., Zawadowicz, M. A., and Bertram, T. H.: Contribution of Speciated Monoterpenes to Secondary Aerosol in the Eastern North Atlantic, ACS EST Air, 1, 789–800, https://doi.org/10.1021/acsestair.3c00112, 2024.

Kilgour, D. B., Jernigan, C. M., Garmash, O., Aggarwal, S., Zhou, S., Mohr, C., Salter, M. E., Thornton, J. A., Wang, J., Zieger, P., and Bertram, T. H.: Cloud processing of dimethyl sulfide (DMS) oxidation products limits sulfur dioxide (SO_2) and carbonyl sulfide (OCS) production in the eastern North Atlantic marine boundary layer, Atmos. Chem. Phys., 25, 1931–1947, https://doi.org/10.5194/acp-25-1931-2025, 2025.

Kim, M. J., Zoerb, M. C., Campbell, N. R., Zimmermann, K. J., Blomquist, B. W., Huebert, B. J., and Bertram, T. H.: Revisiting benzene cluster cations for the chemical ionization of dimethyl sulfide and select volatile organic compounds, Atmos. Meas. Tech., 9, 1473–1484, https://doi.org/10.5194/amt-9-1473-2016, 2016.

Krechmer, J., Lopez-Hilfiker, F., Koss, A., Hutterli, M., Stoermer, C., Deming, B., Kimmel, J., Warneke, C., Holzinger, R., Jayne, J., Worsnop, D., Fuhrer, K., Gonin, M., and de Gouw, J.: Evaluation of a New Reagent-Ion Source and Focusing Ion–Molecule Reactor for Use in Proton-Transfer-Reaction Mass Spectrometry, Anal. Chem., 90, 12011–12018, https://doi.org/10.1021/acs.analchem.8b02641, 2018.

Kremser, S., Thomason, L. W., von Hobe, M., Hermann, M., Deshler, T., Timmreck, C., Toohey, M., Stenke, A., Schwarz, J. P., Weigel, R., Fueglistaler, S., Prata, F. J., Vernier, J.-P., Schlager, H., Barnes, J. E., Antuña-Marrero, J.-C., Fairlie, D., Palm, M., Mahieu, E., Notholt, J., Rex, M., Bingen, C., Vanhellemont, F., Bourassa, A., Plane, J. M. C., Klocke, D., Carn, S. A., Clarisse, L., Trickl, T., Neely, R., James, A. D., Rieger, L., Wilson, J. C., and Meland, B.: Stratospheric aerosol—Observations, processes, and impact on climate, Rev. Geophys., 54, 278–335, https://doi.org/10.1002/2015RG000511, 2016.

Lawson, S. J., Law, C. S., Harvey, M. J., Bell, T. G., Walker, C. F., de Bruyn, W. J., and Saltzman, E. S.: Methanethiol, dimethyl sulfide and acetone over biologically productive waters in the southwest Pacific Ocean, Atmos. Chem. Phys., 20, 3061–3078, https://doi.org/10.5194/acp-20-3061-2020, 2020.

https://doi.org/10.5194/egusphere-2026-5120
Preprint. Discussion started: 24 September 2026

Lennartz, S. T., Marandino, C. A., von Hobe, M., Cortes, P., Quack, B., Simo, R., Booge, D., Pozzer, A., Steinhoff, T., Arevalo-Martinez, D. L., Kloss, C., Bracher, A., Röttgers, R., Atlas, E., and Krüger, K.: Direct oceanic emissions unlikely to account for the missing source of atmospheric carbonyl sulfide, Atmos. Chem. Phys., 17, 385–402, https://doi.org/10.5194/acp-17-385-2017, 2017.

Lennartz, S. T., Marandino, C. A., von Hobe, M., Andreae, M. O., Aranami, K., Atlas, E., Berkelhammer, M., Bingemer, H., Booge, D., Cutter, G., Cortes, P., Kremser, S., Law, C. S., Marriner, A., Simó, R., Quack, B., Uher, G., Xie, H., and Xu, X.: Marine carbonyl sulfide (OCS) and carbon disulfide (CS_2): a compilation of measurements in seawater and the marine boundary layer, Earth Syst. Sci. Data, 12, 591–609, https://doi.org/10.5194/essd-12-591-2020, 2020.

Lennartz, S. T., Simon, H., Booge, D., Zhou, L., and Marandino, C.: CS_2 Cycling in Seawater: Dark Production and UV Light Driven Consumption, Geophys. Res. Lett., 51, e2023GL107024, https://doi.org/10.1029/2023GL107024, 2024.

Linstrom, P. J. and Mallard, W. G. (Eds.): NIST Chemistry WebBook, NIST Standard Reference Database Number 69, https://doi.org/https://webbook.nist.gov/chemistry/, n.d.

Norman, M., Hansel, A., and Wisthaler, A.: O_2^+ as reagent ion in the PTR-MS instrument: Detection of gas-phase ammonia, Int. J. Mass Spectrom., 265, 382–387, https://doi.org/10.1016/j.ijms.2007.06.010, 2007.

Novak, G. A., Kilgour, D. B., Jernigan, C. M., Vermeuel, M. P., and Bertram, T. H.: Oceanic emissions of dimethyl sulfide and methanethiol and their contribution to sulfur dioxide production in the marine atmosphere, Atmos. Chem. Phys., 22, 6309–6325, https://doi.org/10.5194/acp-22-6309-2022, 2022.

Remaud, M., Chevallier, F., Maignan, F., Belviso, S., Berchet, A., Parouffe, A., Abadie, C., Bacour, C., Lennartz, S., and Peylin, P.: Plant gross primary production, plant respiration and carbonyl sulfide emissions over the globe inferred by atmospheric inverse modelling, Atmos. Chem. Phys., 22, 2525–2552, https://doi.org/10.5194/acp-22-2525-2022, 2022.

Rogers, M. N. and Bertram, T. H.: Measurements of Speciated Terpenoids in Chicago, Illinois: An Outsized Role for Anthropogenic Emissions of Monoterpenes, ACS EST Air, 2, 2263–2274, https://doi.org/10.1021/acsestair.5c00215, 2025.

Sandoval-Soto, L., Stanimirov, M., von Hobe, M., Schmitt, V., Valdes, J., Wild, A., and Kesselmeier, J.: Global uptake of carbonyl sulfide (COS) by terrestrial vegetation: Estimates corrected by deposition velocities normalized to the uptake of carbon dioxide (CO_2), Biogeosciences, 2, 125–132, https://doi.org/10.5194/bg-2-125-2005, 2005.

Sheng, J.-X., Weisenstein, D. K., Luo, B.-P., Rozanov, E., Stenke, A., Anet, J., Bingemer, H., and Peter, T.: Global atmospheric sulfur budget under volcanically quiescent conditions: Aerosol-chemistry-climate model predictions and validation, J. Geophys. Res. Atmos., 120, 256–276, https://doi.org/10.1002/2014JD021985, 2015.

https://doi.org/10.5194/egusphere-2026-5120
Preprint. Discussion started: 24 September 2026

Turner, S. M. and Liss, P. S.: Measurements of various sulphur gases in a coastal marine environment, J. Atmos. Chem., 2, 223–232, https://doi.org/10.1007/BF00051074, 1985.

Vermeuel, M. P., Novak, G. A., Kilgour, D. B., Claflin, M. S., Lerner, B. M., Trowbridge, A. M., Thom, J., Cleary, P. A., Desai, A. R., and Bertram, T. H.: Observations of biogenic volatile organic compounds over a mixed temperate forest during the summer to autumn transition, Atmos. Chem. Phys., 23, 4123–4148, https://doi.org/10.5194/acp-23-4123-2023, 2023.

Watts, S. F.: The mass budgets of carbonyl sulfide, dimethyl sulfide, carbon disulfide and hydrogen sulfide, Atmos. Environ., 34, 761–779, https://doi.org/10.1016/S1352-2310(99)00342-8, 2000.

Xie, H., Moore, R. M., and Miller, W. L.: Photochemical production of carbon disulphide in seawater, J. Geophys. Res. Oceans, 103, 5635–5644, https://doi.org/10.1029/97JC02885, 1998.

Xie, H., Scarratt, M. G., and Moore, R. M.: Carbon disulphide production in laboratory cultures of marine phytoplankton, Atmos. Environ., 33, 3445–3453, https://doi.org/10.1016/S1352-2310(98)00430-0, 1999.